

FORMULATION AND IMPLEMENTATION OF NONLINEAR ELASTICITY IN ADVANCED CONSTITUTIVE MODELS IN GEOMECHANICS

TEREZA ŽALSKÁ^{a,*}, MICHAL ŠEJNOHA^b, TOMÁŠ JANDA^b, ALENA ZEMANOVÁ^a

^a Czech Technical University in Prague, Faculty of Civil Engineering, Department of Geotechnics, Thákurova 7, 166 29 Prague, Czech Republic

^b Czech Technical University in Prague, Faculty of Civil Engineering, Department of Mechanics, Thákurova 7, 166 29 Prague, Czech Republic

* corresponding author: tereza.zalska@fsv.cvut.cz

ABSTRACT. Several formulations of a nonlinear elastic behavior within the yield surface of the selected advanced constitutive models are described and compared. Since concentrating on geotechnical applications the accompanied numerical simulations are limited to basic laboratory tests such as isotropic compression, oedometer, and drained triaxial compression. The results show a significant influence of the size of the initial load step on final predictions particularly when starting from a very low initial stiffness associated with the assumed zero initial stress. Differences in the predicted response arising from different formulations are also discussed. These might be quite significant and the design engineer should be aware of that when choosing a particular computational software.

KEYWORDS: Hardening soil model, generalized cam clay model, soft soil model, nonlinear elasticity, oedometer, isotropic compression, triaxial compression.

1. INTRODUCTION

Constructing underground structures in densely populated areas, preventing large scale landslides, as well as being able to accurately simulate a complex response of soils observed experimentally, opens the door to the application of advanced constitutive models [1, 2]. Grounding on experimental evidence such models attempt to address a nonlinear response of soils already at initial stages of loading. An illustrative example are the critical state models [1, 3] where the nonlinear stress-strain behavior within the yield surface arises naturally. A large group of formulations introduce such a behavior in the spirit of Duncan and Chang hyperbolic model [4–7]. While their appearance in available commercial software is common [8–10] (to cite a few), the details on their numerical implementation within a given constitutive model may differ. This in turn may result in predictions, which are considerably influenced by the initial load increment. In some formulations, the load step dependence yields loading-unloading curves which deviate even for loading conditions that do not exceed the yield limit, often resulting in an artificial residual strain. It is therefore crucial to understand such potential drawbacks and the user should be aware of that when creating the computational model for a given geotechnical construction.

The present paper revisits this issue in light of three popular constitutive models implemented in the above mentioned commercial codes. In particular, the Hardening Soil Model [5, 6], the Generalized Cam clay model [10, 11], and the Soft soil model [12] are examined in Section 2 with emphasis on the implementation

of the associated nonlinear elastic constitutive model. The results of numerical simulations together with a thorough discussion are presented in Section 3. All calculations are carried out using the GEO5 FEM software [10].

2. ADVANCED CONSTITUTIVE MODELS

The present section provides details on the formulation of nonlinear elasticity of the selected constitutive models, while the plasticity issues will be presented only briefly with details available in the above mentioned references.

2.1. HARDENING SOIL MODEL

The Hardening soil (HS) model developed in [5] and later extended in [6] to account for small strain yielding is plotted in Figure 1. As seen in Figure 1a it combines two yield surfaces where the shear part, bounded by a limiting yield surface of the Mohr-Coulomb type, is derived on the assumption of the hyperbolic stress-strain response in triaxial compression as depicted in Figure 1c with ε_1 being the major principal strain and q representing an equivalent deviatoric stress measure. In the formulation implemented in GEO5 FEM, both the shear yield surface and the cap yield surface, which is assumed elliptic and centered at the origin of the meridian plane, plot as a smooth hexagon in the deviatoric plane in the spirit of the Matsuoka-Nakai (MN) yield surface [13], see Figure 1b. The evolution (hardening) of both surfaces is controlled by the current value of the equivalent deviatoric plastic strain γ and preconsolidation pressure p_c , respectively.

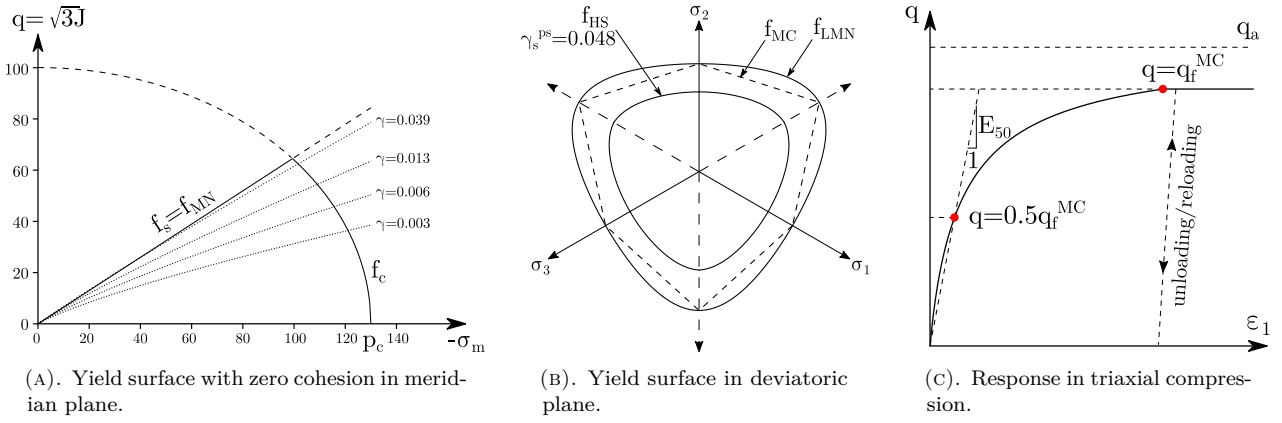


FIGURE 1. Graphical representation of Hardening soil model.

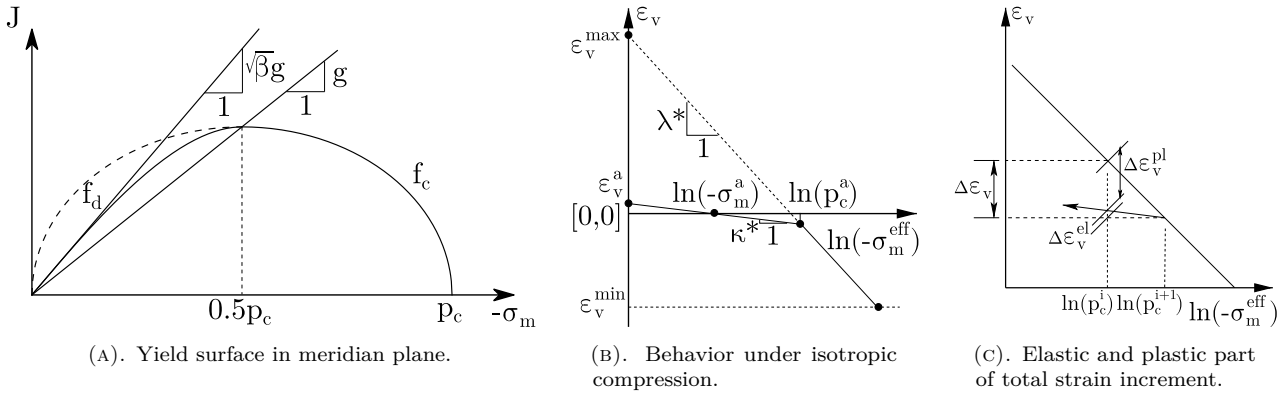


FIGURE 2. Graphical representation of Generalized Cam clay model.

The nonlinear elastic model due to Vermeer [14] writes the elastic modulus E_{ur} in the form of a power law as a function of the current value of mean effective stress σ_m as:

$$E_{ur}(\sigma_m) = E_{ur}^{\text{ref}} \left(\frac{\sigma_m - c \cot \varphi}{\sigma_m^{\text{ref}} - c \cot \varphi} \right)^m, \quad (1)$$

where

E_{ur}^{ref} , σ_m^{ref} , m are model parameters,

c , φ are the shear strength parameters, the cohesion and the angle of internal friction, respectively.

In particular, E_{ur}^{ref} is the reference elastic modulus for a reference stress σ_m^{ref} typically equal to -100 kPa. Note that the standard elasticity sign convention is adopted with tension being positive. For simplicity, we shall now consider the volumetric response only and assume a linear variation of the mean stress σ_m over a given load increment as:

$$\sigma_m = \eta \sigma_m^i + (1 - \eta) \sigma_m^{i+1}. \quad (2)$$

Setting $\eta = 1$ gives fully explicit formulation (forward Euler (FE) method, $\sigma_m = \sigma_m^i$ in Equation (1)) while $\eta = 0$ renders fully implicit (backward Euler (BE) method, $\sigma_m = \sigma_m^{i+1}$ in Equation (1)). Henceforth, the former formulation will be referred to as the constant elasticity (CE) return while the latter formulation will

be termed the variable elasticity (VE) return. Further distinction is made by considering either secant formulation in the form:

$$\sigma_m^{i+1} = K_{ur}(\sigma_m(\eta))(\varepsilon_v^i + \Delta\varepsilon_v), \quad (3)$$

or incremental formulation provided by:

$$\sigma_m^{i+1} = \sigma_m^i + K_{ur}(\sigma_m(\eta))\Delta\varepsilon_v, \quad (4)$$

where K_{ur} is the elastic bulk modulus given by:

$$K_{ur} = \frac{E_{ur}}{3(1 - 2\nu_{ur})}. \quad (5)$$

In particular, cases with $\eta = 1$ (FE), $\eta = 0$ (BE), and so called mid-point rule (MP), i.e., $\eta = 0.5 \rightarrow \sigma_m(\eta) = 0.5(\sigma_m^i + \sigma_m^{i+1})$, will be examined in Section 3.

2.2. GENERALIZED CAM CLAY MODEL

The Generalized Cam clay (GCC) model has been introduced to reconcile the principal drawback of the Modified Cam clay (MCC) model associated with overestimating the shear strength and consequently an excessive softening of highly overconsolidated soils. To this end, the supercritical (dilation) part of the MCC model was suitably adjusted, see Figure 2a, resulting in the dependence on both the critical friction angle φ_{cs} and peak friction angle φ via parameter β given by:

$$\beta = \left(\frac{\sin \varphi}{\sin \varphi_{cs}} \frac{3 - \sin \varphi_{cs}}{3 - \sin \varphi} \right)^2. \quad (6)$$

Similar to the HS model, the MN yield surface represents the projection into a deviatoric plane.

The nonlinear elastic constitutive model derives from the assumed response in isotropic compression shown in Figures 2b and 2c. When moving along the unloading-reloading κ -line the rate form of the stress-strain law is provided by:

$$\dot{\sigma}_m = -\frac{\sigma_m}{\kappa^*} \dot{\varepsilon}_v^{el}, \quad \kappa^* = \frac{\kappa}{1+e}, \quad (7)$$

where

κ is called the swelling modulus,

e is the void ratio.

Integrating over a given time increment gives the evolution of the mean effective stress in the form:

$$\sigma_m^{i+1} = \sigma_m^i \exp \left[\frac{-\Delta \varepsilon_v^{el}}{\kappa^*} \right]. \quad (8)$$

Next, writing the stress increment $\Delta \sigma_m$ as:

$$\begin{aligned} \Delta \sigma_m &= \sigma_m^{i+1} - \sigma_m^i \\ &= \sigma_m^i \left(\exp \left[\frac{-\Delta \varepsilon_v^{el}}{\kappa^*} \right] - 1 \right) = \bar{K}_s \Delta \varepsilon_v^{el}, \end{aligned} \quad (9)$$

allows us to express the secant bulk modulus \bar{K}_s as:

$$\bar{K}_s = \sigma_m^i \frac{\exp \left[\frac{-\Delta \varepsilon_v^{el}}{\kappa^*} \right] - 1}{\Delta \varepsilon_v^{el}}. \quad (10)$$

The analysis may simplify if leaving the concept of variable elasticity return represented by Equation (10) and assume the bulk modulus:

$$K^i = -\frac{\sigma_m^i}{\kappa^*}, \quad (11)$$

to be constant over the load increment (constant elasticity return), recall Equation (7).

2.3. SOFT SOIL MODEL

In the original MCC model the shear strength depends solely on the slope of the critical state line g which for the triaxial compression reads:

$$g = \frac{2\sqrt{3} \sin \varphi_{cs}}{3 - \sin \varphi_{cs}}. \quad (12)$$

Brinkgreve showed in [12] that it is not possible to simulate both the oedometer stress path and full triaxial compression path with good accuracy using the same value of g . This led to the formulation of a Soft soil (SS) model combining the cap yield surface in the form of MCC model to predict a correct K_0 -path and the shear yield surface, here again assumed in the form of MN model, to ensure a correct shear strength. Such a yield surface is plotted in Figure 3 where M_c for triaxial compression is given in terms of the coefficient of lateral earth pressure of normally consolidated

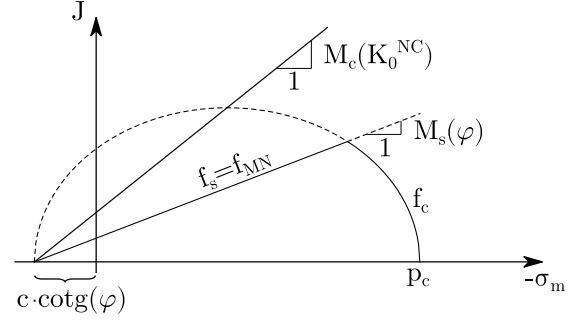


FIGURE 3. Yield surface of Soft soil model in meridian plane.

soils K_0^{NC} [12] whereas M_s follows from the solution of nonlinear MN yield function [13].

While the shear yield surface represents a response of an elastic perfectly plastic material, the cap yield surface may undergo isotropic hardening. To avoid potential softening within the cap model, which is not allowed in the present implementation, the M_c -value should be larger than the slope of the Matsuoka-Nakai failure surface M_s .

Considering the nonlinear elastic response, we follow the implementation in [8] and limit attention to the constant elasticity return of Equation (11). As suggested in [12] it is possible to relate Equation (11) to Equation (1) by writing:

$$K(\sigma_m) = K^{\text{ref}} \left(\frac{\sigma_m}{\sigma_m^{\text{ref}}} \right)^m. \quad (13)$$

When setting $m = 1$, the logarithmic compression law is recovered with:

$$\frac{1}{\kappa^*} = -\frac{K^{\text{ref}}}{\sigma_m^{\text{ref}}}. \quad (14)$$

3. SIMULATION OF SIMPLE LABORATORY TESTS

Numerical simulation of three basic laboratory tests is performed in this section to examine and compare individual formulations presented in the previous section. In all cases, the computational model consists of two constant strain triangular elements. While the oedometer test is run in plane strain regime, the axisymmetric state of stress is assumed for isotropic and triaxial compression. The loading and boundary conditions are displayed in Figure 4 for individual cases. All simulations assumed zero initial stress.

3.1. HARDENING SOIL MODEL

The response in isotropic compression and oedometer is simulated to compare the secant and incremental formulation represented by Equations (3) and (4). As for Equation (2), only the cases with $\eta = 0$ (BE) and $\eta = 0.5$ (MP) are tested. Although purely elastic behavior is addressed, the nonzero values of $c = 10$ kPa and $\varphi = 30^\circ$ are adopted together with $E_{ur}^{\text{ref}} = 30$ MPa

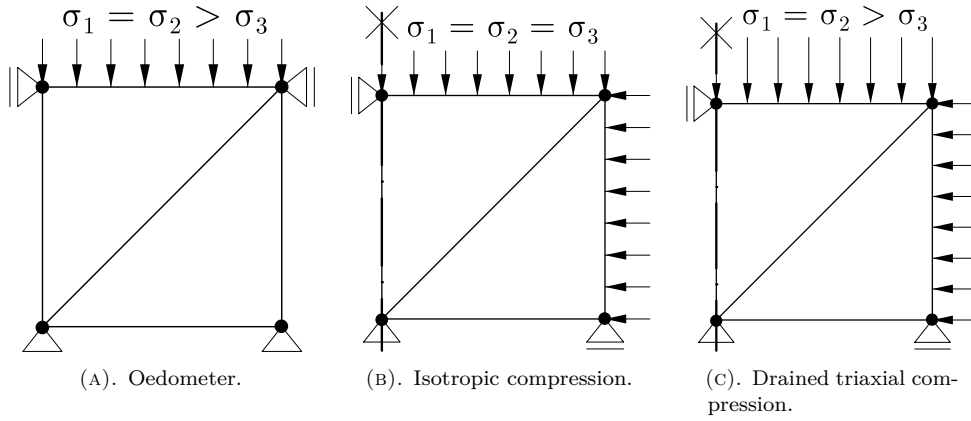


FIGURE 4. Computational models of simple laboratory tests.

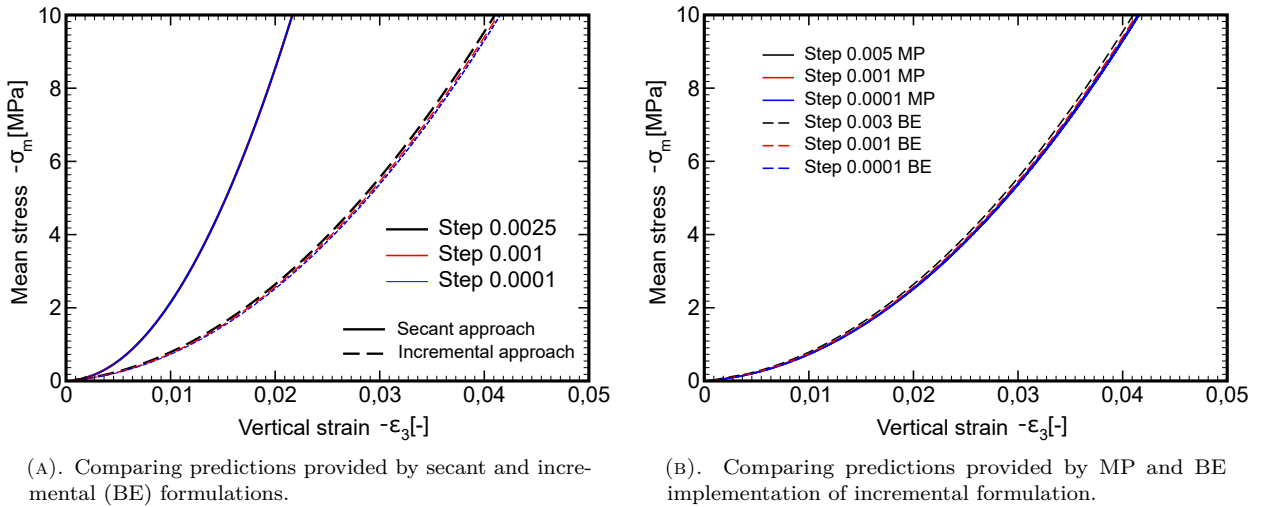


FIGURE 5. Response of HS model in isotropic compression.

and $\sigma_m^{\text{ref}} = -100 \text{ kPa}$ to set the initial stiffness of $E_{ur}(\sigma_m = 0)$ according to Equation (1).

The results for isotropic compression appear in Figure 5. Point out that achieving convergence of the underlying nonlinear equation with $\bar{\sigma}_m(\eta)$ provided by Equations (2)–(4):

$$R = \sigma_m^{i+1} - \bar{\sigma}_m(\eta), \quad (15)$$

required a relatively small initial load increment. So only a minor difference in the nonlinear elastic response is observed for incremental formulation for the tested load steps. On the other, the secant formulation shows response, see Figure 5a, which is step size independent. This conclusion is further supported via results presented in Figure 6a. Point out that both formulations adopt in the present study the same model parameters in the calculation of E_{ur} . However, it is clear from Figure 5a that arriving at identical predictions would require adjusting at minimum the power law coefficient m for individual formulations based on the experimental measurements.

Figure 5b compares the results associated with MP and BE implementation of Equation (1) in the framework of incremental formulation. It appears that MP approach is less sensitive to the size of the loading

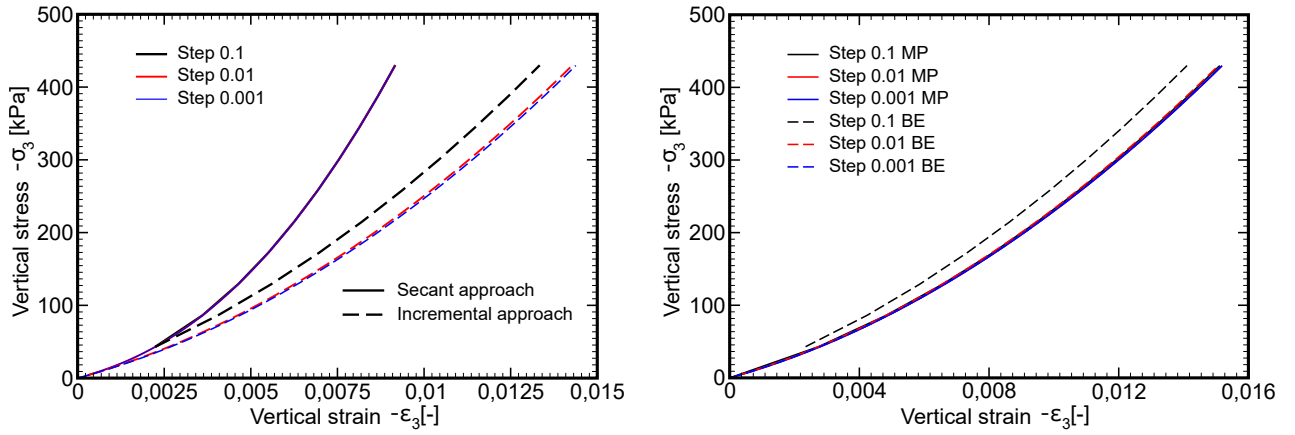
step. This approach is further promoted by predicting an identical stress-strain curve in both loading and unloading if keeping the same load increment. Note that such an approach is implemented in [8] and currently also in [10].

The above discussion is fully supported by simulating an oedometric test as seen in Figure 6. The influence of the load step size, particularly for BE approach, is clearly evident.

3.2. COMPARING GENERALIZED CAM CLAY AND SOFT SOIL MODELS

This section demonstrates potential differences between the variable elasticity approach, adopted with GCC model, and the constant elasticity approach, adopted with SS model, in light of incremental formulation. The material data were set such as to arrive at identical predictions in isotropic compression when enforcing the constant elasticity return also with GCC model. The material parameters used in all subsequent simulations are: $\kappa^* = 0.0094$, $\lambda^* = 0.0678$, $\nu = 0.26$ and $g = M_c = 1.074$. The initial value of $K_0 = \frac{1}{\kappa^*}$ was considered.

Before proceeding with our discussion on individual results it is worth mentioning that the GEO5 FEM



(A). Comparing predictions provided by secant and incremental (BE) formulations.

(B). Comparing predictions provided by MP and BE implementation of incremental formulation.

FIGURE 6. Response of HS model in oedometer.

software allows for gradually increasing the initial size of the load step with a number of iterations needed to achieve global equilibrium. In the present study, the elastic simulations essentially adopted two times larger step size with every new load step when this option, denoted here as VS, was exploited. In this case, the parameter $step_0$, see e.g. Figure 7, represents just the initial step being gradually increased in the course of analysis. All other calculations considered constant step size throughout the analysis.

Exposition to the derived results begins with Figure 7 to show the importance of a relatively small initial load step size to avoid excessive strains attributed to initially very low stiffness.

The influence of stiffness variation over the load increment (VE), Equation (10), in comparison to CE return, Equation (11), appears for isotropic compression in Figure 8. Note that the *-lines require 10 steps only in comparison to 100 and 1000 steps associated with red and blue simulations, respectively.

Promoting VE return over CE return might seem justifiable when leaving purely elastic response and allowing for plasticity as shown in Figure 8b where simulations based on variable step size match those with the constant step size in the case of VE rather well.

Similar conclusions can be drawn from the results in Figure 9 derived for oedometer. Figure 9a further shows that, unlike the HS model, the assumed stiffness evolution leads to artificial residual strains upon complete unloading even in the case of pure elasticity, which may become significant for larger load steps. On the other hand, this issue will become less important when loading the soil beyond its relatively low elastic limit, because the generated permanent plastic strains will then well exceed their elastic counterparts.

The last simulations are concerned with the plastic response predicted by the GCC and SS models for the drained triaxial compression test. As seen in Figure 10 the analysis begins with isotropic compression, Figure 4b, when the specimen is first loaded to acquire

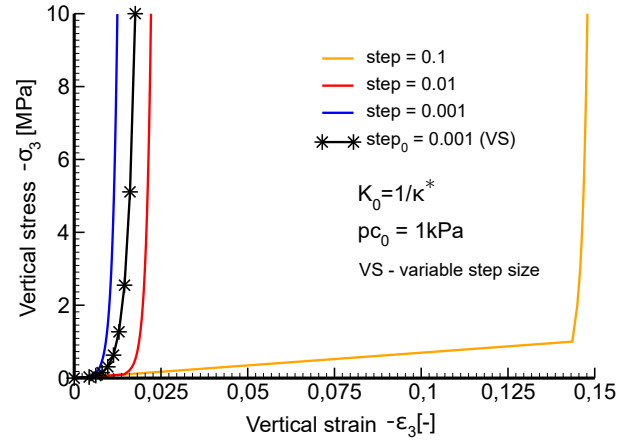


FIGURE 7. Nonlinear elastic response of GCC model in isotropic compression: influence of initial step size.

an initial pressure of 50 kPa. Clearly, no deviatoric stresses are generated during this loading stage. The evolution of deviatoric stresses begins with the second stage of loading corresponding to triaxial compression, Figure 4c. Note that the deviatoric stress measure J is defined as the square root of the 2nd invariant of deviatoric stresses s_{ij} as:

$$J = \sqrt{\frac{1}{2}s_{ij}s_{ij}}. \quad (16)$$

Similarly to previous studies the CE predictions linked to variable step size (VS) slightly deviate from those obtained with the constant step size. This is not the case for the approach based on VE return. However, it is fair to mention, that smooth convergence with VE required a slightly larger number of iterations, thus a smaller load step size, in contrast to CE return (star and diamond symbols identify individual load steps). Also note that for sufficiently small load steps the difference between the two approaches becomes insignificant.

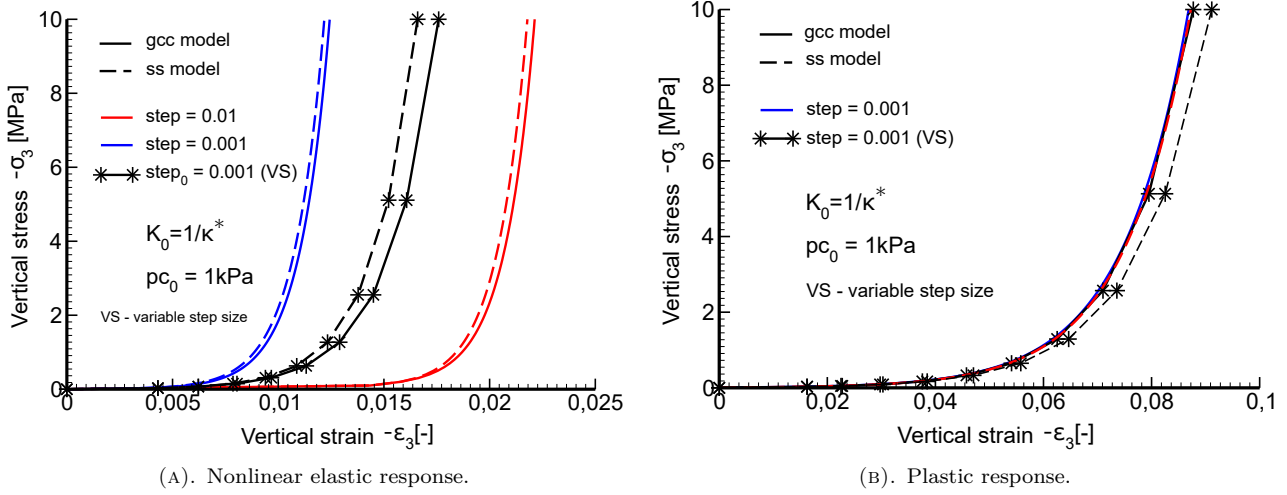


FIGURE 8. Comparing GCC and SS models in isotropic compression.

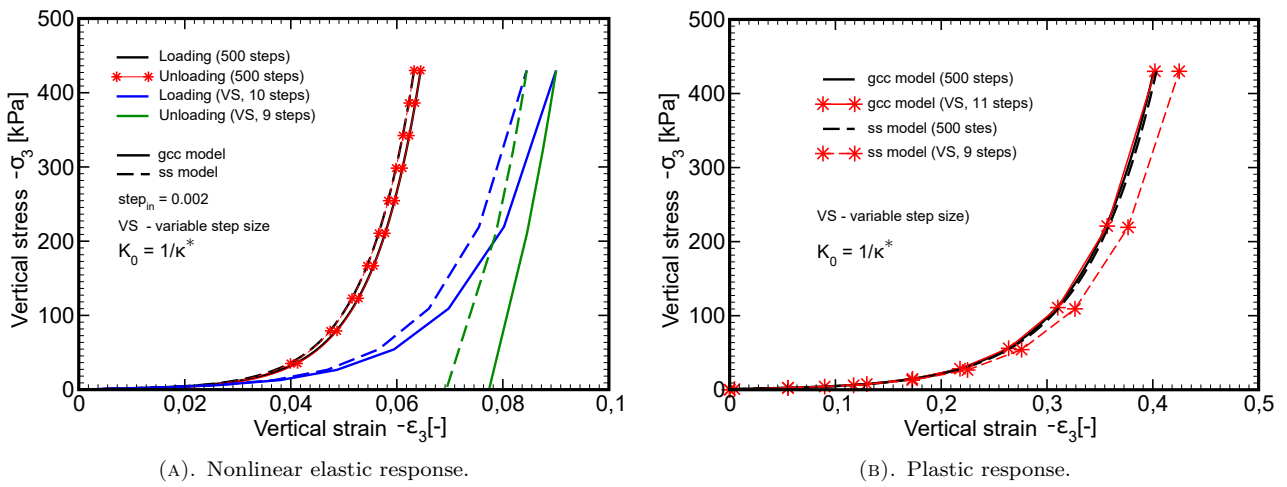


FIGURE 9. Comparing GCC and SS models in oedometer.

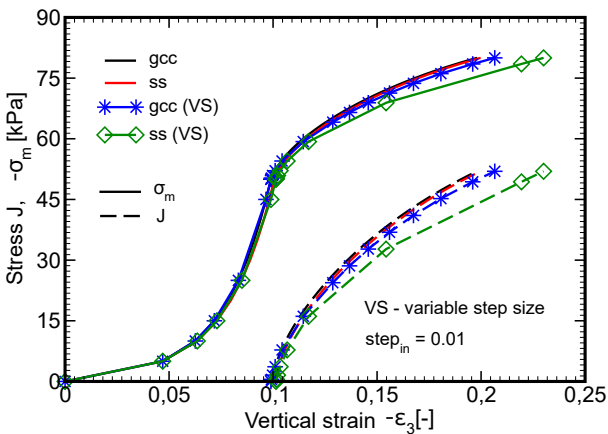


FIGURE 10. Comparing GCC and SS models in drained triaxial compression.

4. CONCLUSION

The paper presented several illustrative examples via simulations of simple laboratory tests to show differences in the implementation of nonlinear elastic constitutive laws arising in the formulation of three particular advanced plasticity models.

It has been confirmed that the chosen method of implementation may considerably affect the predicted response. The user of a given commercial software should be aware of that, since using the same model in different softwares does not assure the same results. Common to all examined models is their dependence on the mean effective stress which may generate a very low initial stiffness when starting from zero initial stress. This in turn leads to excessive strains providing the initial load steps are not sufficiently small. To avoid a large number of loading steps to reach the prescribed load the program GEO5 FEM allows for a gradual increase of the initially small step size in dependence on the number of iterations needed to converge for the previous load increment.

It has also been observed that with the GCC and SS models irreversible elastic strains occur as the stiffness at the end of the loading and at the beginning of unloading is different. On the other hand, this issue does not seem to play a major role as the influence of irreversible elastic strains become negligible in plastic analyses. In this regard, the approach based on variable elasticity return provides response which

seems less dependent on increasing the load step in simulations adopting the variable step size (VS).

To conclude we remind that the GEO5 FEM software, adopts, similar to [8], the incremental formulation with MP approach for the HS model and the concept of constant elasticity return for the SS model. On the other hand, the MCC and GCC models employ the variable elasticity return approach.

ACKNOWLEDGEMENTS

The support provided by the SGS project No. SGS23/032/OHK1/1T/11 and by the GAČR grant No. 22-12178S is gratefully acknowledged.

REFERENCES

- [1] K. H. Roscoe, J. B. Burland. On the generalised stress-strain behaviour of ‘wet’ clay. In J. Heyman, F. A. Lechie (eds.), *Engineering plasticity*, pp. 535–609. Cambridge University Press, 1968.
- [2] D. Mašín. A hypoplastic constitutive models for clays. *International Journal for Numerical and Analytical Methods in Geomechanics* **29**(4):311–336, 2005. <https://doi.org/10.1002/nag.416>
- [3] D. M. Potts, L. Zdravkovič. *Finite element analysis in geotechnical engineering: Volume one – theory*. Thomas Telford Publishing, UK, 1999. <https://doi.org/10.1680/feaiget.27534>
- [4] J. M. Duncan, C.-Y. Chang. Nonlinear analysis of stress and strain in soils. *Journal of the Soil Mechanics and Foundations Division* **96**(5):1629–1653, 1970. <https://doi.org/10.1061/JSFEAQ.0001458>
- [5] T. Schanz, P. A. Vermeer, P. G. Bonnier. The hardening soil model: Formulation and verification. In R. B. J. Brinkgreve (ed.), *Beyond 2000 in Computational Geotechnics*, pp. 281–290. 1999. <https://doi.org/10.1201/9781315138206-27>
- [6] T. Benz. *Small-strain stiffness of soils and its numerical consequences*. Ph.D. thesis, University of Stuttgart, 2007.
- [7] J. Veselý. *The use of the advanced material models for the numerical modelling of the underground structures in clays*. Ph.D. thesis, CTU in Prague, Faculty of Civil Engineering, 2016.
- [8] Seequent.com. PLAXIS. [2023-11-03]. <http://www.plaxis.nl/>
- [9] ZSOIL. [2023-11-03]. <http://www.zsoil.com/>
- [10] Fine.cz. GEO5 FEM. [2023-11-03]. <http://www.fine.cz/>
- [11] T. Janda, M. Šejnoha. Formulation of generalized Cam clay model. *Engineering Mechanics* **13**(5):367–384, 2006.
- [12] R. B. J. Brinkgreve. *Geomaterial model and numerical analysis of softening*. Ph.D. thesis, Delft University of Technology, 1994.
- [13] J. P. Bardet. Lode dependences for isotropic pressure-sensitive elastoplastic materials. *Journal of Applied Mechanics* **57**(3):498–506, 1990. <https://doi.org/10.1115/1.2897051>
- [14] P. A. Vermeer. *Formulation and analysis of sand deformation problems*. Ph.D. thesis, Delft University of Technology, 1980.